

184122: metamorphosed quartz sandstone, Plum Pudding Rocks

(*Coramup Gneiss, Biranup Complex, Albany–Fraser Orogen*)

Location and sampling

ESPERANCE (SI 51-6), ESPERANCE (3230)
MGA Zone 51, 377419E 6251030N

Sampled on 21 May 2006

The sample was collected from a low outcrop near the top of a large, eastward-sloping rock platform that is part of the coastal exposure at Plum Pudding Rocks, about 30 m northwest of GSWA 184123 (Bodorkos and Wingate, 2008).

Tectonic unit/relations

The unit sampled is a pale grey, coarse-grained and garnet-bearing metamorphosed quartz sandstone attributed to the Coramup Gneiss within the Biranup Complex of the Albany–Fraser Orogen (Myers, 1995). The metasandstone is interlayered with metapelitic rocks at 1–10 m-scale, and both contain a gneissosity that is axially planar to small-scale intrafolial folds. This fabric is absent from the adjacent garnet-bearing monzogranitic gneiss (of which GSWA 184123 (Bodorkos and Wingate, 2008) is representative), which suggests that the precursor monzogranite intruded the protoliths of the metasedimentary rocks, but the relative timing relationships are not clear. The monzogranitic gneiss contains a well-developed differentiated layering (Bodorkos and Wingate, 2008), and all rocks and fabrics are affected by mesoscopic to macroscopic upright tight folds that plunge gently to the northeast and southwest.

Petrographic description

The visually estimated primary mineralogy of this sample is dominated by quartz (85%), with subordinate plagioclase (10%), biotite (2%), garnet (2%), and accessory zircon. The overall texture is granoblastic: quartz occurs as interlocking anhedral grains up to 10 mm in diameter, and is intergrown with disseminated plagioclase up to 10 mm in size that has been irregularly altered to sericite. A foliation is defined by oriented grains of biotite (now altered to clay minerals, leucoxene, and limonite), with which rare garnet (mostly fresh, but with some muscovite- and limonite-filled fractures) up to 2.5 mm in diameter is associated. Most quartz c-axes are at a low angle to the foliation. Sparse zircon occurs as rounded crystals up to 0.15 mm in diameter.

The granoblastic texture and exaggerated growth of quartz grains in the sample is consistent with

recrystallization under upper amphibolite to granulite facies conditions. The development of sericite, muscovite, limonite, and clay minerals is consistent with alteration or retrograde metamorphism under lower greenschist facies conditions.

Zircon morphology

Zircons isolated from this sample are mainly euhedral to subhedral and rounded, and range from clear and colourless, through pale brown and turbid, to dark brown and opaque. They are up to 600 μm long, with aspect ratios up to 5:1, although several broken crystals were originally larger. Many grains are strongly cracked. A cathodoluminescence (CL) image of representative zircons is shown in Figure 1. Coarse zoning is common in most zircon cores with high CL emission, and many crystals exhibit thick rims, predominantly as partly-rounded pyramidal terminations, that are clear in transmitted light, but have very low CL emission (Fig. 1). Several zircons show disrupted internal structures, consistent with recrystallization.

Analytical details

This sample was analysed on 20–21 September 2006, using SHRIMP-B. Twenty-two analyses of the Temora standard were obtained during the session, and indicated an external spot-to-spot (reproducibility) uncertainty of 1.57% (1 σ) and a $^{238}\text{U}/^{206}\text{Pb}^*$ calibration uncertainty of 0.38% (1 σ). Common-Pb corrections were applied to all analyses using contemporaneous common-Pb isotopic compositions determined according to the model of Stacey and Kramers (1975).

Results

Seventy-three analyses were obtained from 60 zircons, with 13 grains (2, 5–6, 8, 10–11, 14–16, 18–20, and 22) each analysed twice. Results are listed in Table 1, and shown in a concordia diagram (Fig. 2), and a probability density diagram (Fig. 3).

Interpretation

The analyses range from slightly reversely to moderately normally discordant (Fig. 2). Eight analyses are moderately discordant (>10%): the dates obtained from these analyses (Group D; Table 1) are imprecise or unreliable, and are

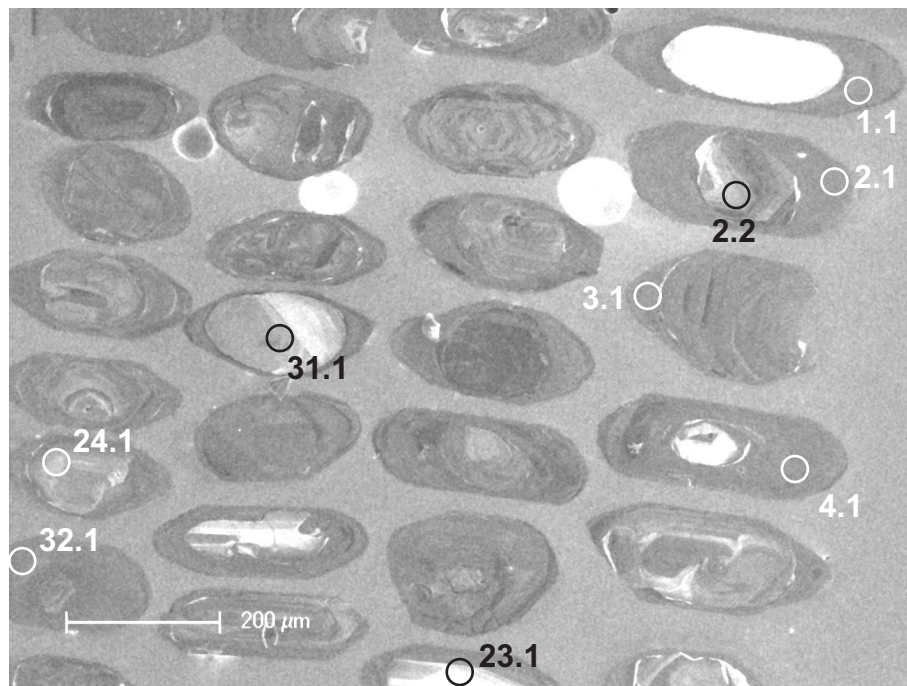


Figure 1. Cathodoluminescence image of representative zircons from sample 184122: metamorphosed quartz sandstone, Plum Pudding Rocks. Numbered circles indicate the approximate positions of analysis sites

not considered geologically significant. The remaining 65 analyses can be divided into five groups based on their positions within the grains, their uranium contents, and their Th/U and $^{207}\text{Pb}^*/^{206}\text{Pb}^*$ ratios.

Group 1 comprises 11 analyses of 11 zircon rims (Table 1) with high uranium content (443–800 ppm) and low Th/U (0.03–0.06), which yield a weighted mean $^{207}\text{Pb}^*/^{206}\text{Pb}^*$ date of 1225 ± 7 Ma (MSWD = 1.8).

Group 2 comprises a single analysis of a zircon core (Table 1) with a low uranium content (62 ppm) and high Th/U (1.03), which yields a $^{207}\text{Pb}^*/^{206}\text{Pb}^*$ date of 1757 ± 39 Ma (1σ).

Group 3 comprises 36 analyses of 36 zircon cores (Table 1) with low to moderate uranium content (44–424 ppm) and widely varied Th/U (0.11–1.63), which yield $^{207}\text{Pb}^*/^{206}\text{Pb}^*$ dates of 3392–2020 Ma.

Group 4 comprises 16 analyses of 16 zircon rims (Table 1) with high uranium content (408–746 ppm) and low Th/U (0.03–0.10), which yield a weighted mean $^{207}\text{Pb}^*/^{206}\text{Pb}^*$ date of 1196 ± 7 Ma (MSWD = 1.6).

Group 5 comprises a single analysis of a zircon rim (Table 1) with a moderate uranium content (461 ppm) and low Th/U (0.04), which yields a $^{207}\text{Pb}^*/^{206}\text{Pb}^*$ date of 1271 ± 13 Ma (1σ).

The date of 1225 ± 7 Ma for the 11 rim analyses in Group 1 is interpreted as the age of the high-grade metamorphic event responsible for zircon rim growth in the metamorphosed quartz sandstone.

The date of 1757 ± 39 Ma (1σ) for the single analysis (14.2; Table 1) in Group 2 is interpreted as the age of the youngest detrital zircon core, and therefore constitutes a maximum age for deposition of the quartz sandstone. The 36 core analyses in Group 3 have $^{207}\text{Pb}^*/^{206}\text{Pb}^*$ dates that define significant age components (based on three or more data points) at c. 2031, 2263, 2357, 2623, and 2650 Ma, and several minor components spanning the range 3392–2102 Ma (Fig. 3). These are interpreted as the ages of zircon-bearing rocks in the detrital source region(s) of the quartz sandstone.

The 16 analyses in Group 4 are interpreted as metamorphic zircon rims affected by minor ancient loss of radiogenic Pb. The date of 1196 ± 7 Ma defined by the 16 analyses constitutes a maximum age for the Pb-loss event, which may have been related to the c. 1170 Ma tectonothermal event documented at this locality by Bodorkos and Clark (2004). The single analysis in Group 5 (3.1; Table 1) is interpreted to be of a metamorphic zircon rim that has incorporated a small amount of material from the inner core, and its date of 1271 ± 13 Ma (1σ) is not accorded any geological significance.

An independent constraint for the minimum age for deposition of the quartz sandstone is provided by the igneous crystallization age of 1688 ± 12 Ma for the precursor of the garnet-bearing monzogranitic gneiss (GSWA 184123; Bodorkos and Wingate, 2008) that is interpreted to intrude the metamorphosed quartz sandstone at this locality. In addition, the date of 1225 ± 7 Ma ascribed to high-grade metamorphism of the quartz sandstone is indistinguishable from the date of 1224 ± 9 Ma attributed to high-grade metamorphism of

Table 1. Ion microprobe analytical results for zircons from sample 184122: metamorphosed quartz sandstone, Plum Pudding Rocks

Grp no.	Spot no.	Grain .spot	^{238}U (ppm)	^{232}Th (ppm)	$\frac{^{232}\text{Th}}{^{238}\text{U}}$	f^{204} (%)	$^{238}\text{U}/^{206}\text{Pb}$ $\pm 1\sigma$	$^{207}\text{Pb}/^{206}\text{Pb}$ $\pm 1\sigma$	$^{238}\text{U}/^{206}\text{Pb}^*$ $\pm 1\sigma$	$^{207}\text{Pb}^*/^{206}\text{Pb}^*$ $\pm 1\sigma$	$^{238}\text{U}/^{206}\text{Pb}^*$ date (Ma) $\pm 1\sigma$	$^{207}\text{Pb}^*/^{206}\text{Pb}^*$ date (Ma) $\pm 1\sigma$	D_{isc} (%)
1	4	4.1	800	24	0.03	0.002	4.807 \pm 0.078	0.08176 \pm 0.00023	4.807 \pm 0.078	0.08174 \pm 0.00024	1218 \pm 18	1239 \pm 6	1.7
1	6	6.1	511	22	0.04	0.020	4.797 \pm 0.077	0.08190 \pm 0.00029	4.798 \pm 0.077	0.08173 \pm 0.00032	1221 \pm 18	1239 \pm 8	1.5
1	16	16.1	443	19	0.04	0.002	4.912 \pm 0.080	0.08135 \pm 0.00035	4.912 \pm 0.080	0.08133 \pm 0.00037	1195 \pm 18	1230 \pm 9	2.8
1	20	20.1	608	27	0.05	0.020	4.872 \pm 0.077	0.08138 \pm 0.00031	4.873 \pm 0.077	0.08122 \pm 0.00033	1203 \pm 17	1227 \pm 8	1.9
1	18	18.1	611	29	0.05	-0.003	4.830 \pm 0.077	0.08112 \pm 0.00026	4.830 \pm 0.077	0.08115 \pm 0.00026	1213 \pm 18	1225 \pm 6	1.0
1	41	28.1	737	30	0.04	0.010	4.821 \pm 0.077	0.08122 \pm 0.00025	4.822 \pm 0.077	0.08114 \pm 0.00027	1215 \pm 18	1225 \pm 6	0.8
1	12	12.1	468	25	0.06	0.021	4.847 \pm 0.077	0.08114 \pm 0.00029	4.848 \pm 0.077	0.08096 \pm 0.00032	1209 \pm 18	1221 \pm 8	0.9
1	2	2.1	566	22	0.04	0.023	4.809 \pm 0.077	0.08105 \pm 0.00029	4.810 \pm 0.077	0.08085 \pm 0.00031	1218 \pm 18	1218 \pm 7	0.0
1	40	27.1	546	25	0.05	0.028	4.841 \pm 0.084	0.08102 \pm 0.00042	4.843 \pm 0.084	0.08078 \pm 0.00043	1210 \pm 19	1216 \pm 11	0.5
1	19	19.1	557	31	0.06	0.015	4.894 \pm 0.078	0.08075 \pm 0.00027	4.895 \pm 0.078	0.08062 \pm 0.00029	1198 \pm 18	1212 \pm 7	1.1
1	5	5.1	502	21	0.04	0.028	4.915 \pm 0.078	0.08080 \pm 0.00033	4.916 \pm 0.078	0.08057 \pm 0.00036	1194 \pm 17	1211 \pm 9	1.4
2	31	14.2	62	62	1.03	0.201	3.038 \pm 0.077	0.10924 \pm 0.00214	3.044 \pm 0.077	0.10749 \pm 0.00230	1831 \pm 41	1757 \pm 39	-4.2
3	35	19.2	100	113	1.17	0.107	2.635 \pm 0.045	0.12532 \pm 0.00075	2.638 \pm 0.045	0.12437 \pm 0.00084	2072 \pm 30	2020 \pm 12	-2.6
3	50	37.1	424	302	0.74	0.045	2.743 \pm 0.045	0.12536 \pm 0.00048	2.744 \pm 0.045	0.12497 \pm 0.00050	2003 \pm 28	2028 \pm 7	1.3
3	55	42.1	404	120	0.31	0.044	2.468 \pm 0.060	0.12596 \pm 0.00051	2.469 \pm 0.060	0.12557 \pm 0.00054	2192 \pm 45	2037 \pm 8	-7.6
3	26	5.2	370	109	0.30	0.021	2.436 \pm 0.039	0.12917 \pm 0.00144	2.436 \pm 0.039	0.12898 \pm 0.00145	2217 \pm 30	2084 \pm 20	-6.4
3	62	49.1	76	120	1.63	0.034	2.613 \pm 0.046	0.13108 \pm 0.00111	2.614 \pm 0.046	0.13079 \pm 0.00118	2088 \pm 31	2109 \pm 16	1.0
3	73	60.1	235	160	0.70	0.017	2.437 \pm 0.040	0.13528 \pm 0.00141	2.437 \pm 0.040	0.13513 \pm 0.00141	2216 \pm 31	2166 \pm 18	-2.3
3	52	39.1	177	55	0.32	0.111	2.419 \pm 0.040	0.14370 \pm 0.00122	2.422 \pm 0.041	0.14271 \pm 0.00128	2228 \pm 32	2260 \pm 15	1.4
3	57	44.1	95	113	1.23	0.021	2.234 \pm 0.038	0.14428 \pm 0.00320	2.235 \pm 0.038	0.14410 \pm 0.00320	2384 \pm 34	2277 \pm 38	-4.7
3	37	22.2	267	67	0.26	0.105	2.445 \pm 0.040	0.14647 \pm 0.00303	2.447 \pm 0.040	0.14554 \pm 0.00305	2209 \pm 31	2294 \pm 36	3.7
3	34	18.2	59	33	0.59	0.094	2.147 \pm 0.049	0.14926 \pm 0.00156	2.149 \pm 0.049	0.14842 \pm 0.00166	2463 \pm 47	2328 \pm 19	-5.8
3	66	53.1	261	39	0.15	0.030	2.192 \pm 0.056	0.15104 \pm 0.00176	2.192 \pm 0.056	0.15077 \pm 0.00177	2423 \pm 52	2355 \pm 20	-2.9
3	47	34.1	379	40	0.11	0.009	2.251 \pm 0.036	0.15167 \pm 0.00132	2.251 \pm 0.036	0.15159 \pm 0.00132	2369 \pm 32	2364 \pm 15	-0.2
3	61	48.1	172	64	0.39	0.150	2.327 \pm 0.040	0.15547 \pm 0.00558	2.331 \pm 0.040	0.15414 \pm 0.00560	2301 \pm 33	2392 \pm 62	3.8
3	68	55.1	234	37	0.17	0.011	2.060 \pm 0.034	0.15572 \pm 0.00136	2.060 \pm 0.034	0.15562 \pm 0.00136	2551 \pm 35	2409 \pm 15	-5.9
3	23	2.2	149	56	0.39	0.167	2.243 \pm 0.037	0.16281 \pm 0.00173	2.247 \pm 0.037	0.16132 \pm 0.00178	2373 \pm 33	2470 \pm 19	3.9
3	36	20.2	334	57	0.18	0.008	2.341 \pm 0.046	0.16512 \pm 0.00832	2.341 \pm 0.046	0.16504 \pm 0.00832	2293 \pm 38	2508 \pm 85	8.6
3	65	52.1	100	43	0.44	-0.024	2.141 \pm 0.054	0.16713 \pm 0.00107	2.140 \pm 0.054	0.16734 \pm 0.00107	2471 \pm 52	2531 \pm 11	2.4
3	46	33.1	75	63	0.87	-0.026	2.009 \pm 0.036	0.17035 \pm 0.00335	2.009 \pm 0.036	0.17058 \pm 0.00335	2604 \pm 38	2563 \pm 33	-1.6
3	54	41.1	316	166	0.54	0.001	1.994 \pm 0.032	0.17615 \pm 0.00086	1.994 \pm 0.032	0.17614 \pm 0.00086	2620 \pm 35	2617 \pm 8	-0.1
3	27	6.2	367	70	0.20	0.022	2.111 \pm 0.034	0.17700 \pm 0.00119	2.111 \pm 0.034	0.17680 \pm 0.00119	2500 \pm 33	2623 \pm 11	4.7
3	44	31.1	116	119	1.06	0.048	1.973 \pm 0.034	0.17772 \pm 0.00156	1.974 \pm 0.034	0.17729 \pm 0.00159	2642 \pm 37	2628 \pm 15	-0.5
3	70	57.1	288	96	0.34	0.042	1.884 \pm 0.031	0.17776 \pm 0.00206	1.885 \pm 0.031	0.17739 \pm 0.00206	2744 \pm 37	2629 \pm 19	-4.4
3	49	36.1	424	270	0.66	0.001	1.984 \pm 0.039	0.17753 \pm 0.00115	1.984 \pm 0.039	0.17752 \pm 0.00115	2631 \pm 42	2630 \pm 11	0.0
3	28	8.2	420	226	0.56	0.002	1.918 \pm 0.032	0.17847 \pm 0.00173	1.918 \pm 0.032	0.17845 \pm 0.00173	2705 \pm 36	2639 \pm 16	-2.5
3	67	54.1	320	152	0.49	0.001	2.053 \pm 0.039	0.17957 \pm 0.00081	2.053 \pm 0.039	0.17956 \pm 0.00081	2558 \pm 40	2649 \pm 7	3.4
3	63	50.1	162	70	0.45	-0.021	2.001 \pm 0.033	0.18010 \pm 0.00083	2.000 \pm 0.033	0.18029 \pm 0.00083	2613 \pm 36	2656 \pm 8	1.6
3	53	40.1	166	71	0.44	0.041	1.901 \pm 0.032	0.18190 \pm 0.00188	1.901 \pm 0.032	0.18153 \pm 0.00189	2724 \pm 37	2667 \pm 17	-2.2
3	56	43.1	169	154	0.94	-0.015	1.973 \pm 0.066	0.18282 \pm 0.00537	1.973 \pm 0.066	0.18295 \pm 0.00537	2643 \pm 73	2680 \pm 49	1.4
3	58	45.1	117	124	1.09	-0.026	1.977 \pm 0.034	0.18677 \pm 0.00102	1.976 \pm 0.034	0.18700 \pm 0.00108	2639 \pm 37	2716 \pm 10	2.8
3	30	11.2	72	51	0.74	0.063	1.877 \pm 0.086	0.18788 \pm 0.00339	1.878 \pm 0.086	0.18732 \pm 0.00341	2752 \pm 103	2719 \pm 30	-1.2

Table 1. (continued)

Grp no.	Spot no.	Grain .spot	^{238}U (ppm)	^{232}Th (ppm)	$^{232}\text{Th}/^{238}\text{U}$	f^{204} (%)	$^{238}\text{U}/^{206}\text{Pb}$ $\pm 1\sigma$	$^{207}\text{Pb}/^{206}\text{Pb}$ $\pm 1\sigma$	$^{238}\text{U}/^{206}\text{Pb}^*$ $\pm 1\sigma$	$^{207}\text{Pb}^*/^{206}\text{Pb}^*$ $\pm 1\sigma$	$^{238}\text{U}/^{206}\text{Pb}^*$ date (Ma) $\pm 1\sigma$	$^{207}\text{Pb}^*/^{206}\text{Pb}^*$ date (Ma) $\pm 1\sigma$	D_{isc} (%)
3	71	58.1	47	26	0.57	0.102	2.060 \pm 0.053	0.19358 \pm 0.00166	2.062 \pm 0.053	0.19268 \pm 0.00170	2549 \pm 54	2765 \pm 15	7.8
3	69	56.1	115	47	0.42	0.036	1.985 \pm 0.034	0.19751 \pm 0.00623	1.986 \pm 0.034	0.19719 \pm 0.00624	2629 \pm 37	2803 \pm 52	6.2
3	25	24.1	137	101	0.76	0.008	1.756 \pm 0.029	0.21282 \pm 0.00073	1.756 \pm 0.029	0.21274 \pm 0.00074	2906 \pm 38	2927 \pm 6	0.7
3	24	23.1	44	15	0.36	-0.008	1.698 \pm 0.063	0.25582 \pm 0.00513	1.698 \pm 0.063	0.25590 \pm 0.00513	2985 \pm 88	3222 \pm 32	7.3
3	33	16.2	283	228	0.83	-0.002	1.578 \pm 0.026	0.25806 \pm 0.00100	1.578 \pm 0.026	0.25808 \pm 0.00100	3164 \pm 41	3235 \pm 6	2.2
3	64	51.1	317	239	0.78	0.002	1.477 \pm 0.024	0.28528 \pm 0.00088	1.477 \pm 0.024	0.28526 \pm 0.00088	3332 \pm 42	3392 \pm 5	1.8
4	10	10.1	627	27	0.04	0.075	4.740 \pm 0.078	0.08118 \pm 0.00025	4.743 \pm 0.078	0.08054 \pm 0.00033	1233 \pm 18	1210 \pm 8	-1.9
4	13	13.1	746	42	0.06	0.123	5.149 \pm 0.082	0.08148 \pm 0.00035	5.155 \pm 0.082	0.08044 \pm 0.00041	1143 \pm 17	1208 \pm 10	5.4
4	7	7.1	543	23	0.04	0.003	4.824 \pm 0.077	0.08045 \pm 0.00028	4.824 \pm 0.077	0.08043 \pm 0.00028	1214 \pm 18	1207 \pm 7	-0.6
4	45	32.1	477	45	0.10	0.048	4.901 \pm 0.079	0.08082 \pm 0.00045	4.903 \pm 0.079	0.08042 \pm 0.00047	1197 \pm 18	1207 \pm 12	0.9
4	42	29.1	485	21	0.04	0.084	5.035 \pm 0.081	0.08112 \pm 0.00032	5.040 \pm 0.081	0.08041 \pm 0.00040	1167 \pm 17	1207 \pm 10	3.3
4	8	8.1	602	33	0.06	0.140	4.897 \pm 0.081	0.08149 \pm 0.00026	4.904 \pm 0.081	0.08030 \pm 0.00036	1196 \pm 18	1204 \pm 9	0.7
4	39	26.1	449	21	0.05	0.139	5.041 \pm 0.081	0.08141 \pm 0.00033	5.048 \pm 0.081	0.08023 \pm 0.00046	1165 \pm 17	1203 \pm 11	3.1
4	1	1.1	495	22	0.05	0.127	4.922 \pm 0.079	0.08112 \pm 0.00031	4.928 \pm 0.079	0.08005 \pm 0.00040	1191 \pm 17	1198 \pm 10	0.6
4	21	21.1	517	17	0.03	0.294	5.065 \pm 0.081	0.08245 \pm 0.00048	5.080 \pm 0.081	0.07997 \pm 0.00059	1158 \pm 17	1196 \pm 15	3.1
4	38	25.1	447	18	0.04	0.010	4.930 \pm 0.089	0.08002 \pm 0.00064	4.931 \pm 0.089	0.07994 \pm 0.00065	1190 \pm 20	1196 \pm 16	0.4
4	22	22.1	477	25	0.05	0.050	4.971 \pm 0.080	0.08015 \pm 0.00029	4.974 \pm 0.081	0.07973 \pm 0.00035	1181 \pm 17	1190 \pm 9	0.8
4	43	30.1	408	16	0.04	0.048	4.834 \pm 0.077	0.08010 \pm 0.00034	4.837 \pm 0.078	0.07969 \pm 0.00044	1212 \pm 18	1189 \pm 11	-1.9
4	15	15.1	708	47	0.07	0.023	4.899 \pm 0.079	0.07978 \pm 0.00023	4.900 \pm 0.079	0.07958 \pm 0.00026	1197 \pm 18	1187 \pm 6	-0.9
4	11	11.1	693	22	0.03	0.025	5.168 \pm 0.085	0.07963 \pm 0.00028	5.170 \pm 0.086	0.07941 \pm 0.00033	1140 \pm 17	1182 \pm 8	3.6
4	14	14.1	446	34	0.08	0.043	5.049 \pm 0.081	0.07973 \pm 0.00029	5.051 \pm 0.081	0.07936 \pm 0.00038	1165 \pm 17	1181 \pm 9	1.4
4	9	9.1	477	18	0.04	0.098	5.352 \pm 0.085	0.07991 \pm 0.00030	5.357 \pm 0.085	0.07908 \pm 0.00038	1103 \pm 16	1174 \pm 10	6.0
5	3	3.1	461	17	0.04	0.206	4.740 \pm 0.077	0.08482 \pm 0.00043	4.750 \pm 0.077	0.08308 \pm 0.00056	1232 \pm 18	1271 \pm 13	3.1
D	32	15.2	313	74	0.24	-0.026	2.408 \pm 0.040	0.12503 \pm 0.01541	2.407 \pm 0.040	0.12525 \pm 0.01541	2240 \pm 32	2032 \pm 218	-10.2
D	48	35.1	265	58	0.23	-0.024	3.063 \pm 0.051	0.12799 \pm 0.00442	3.062 \pm 0.051	0.12820 \pm 0.00442	1822 \pm 27	2073 \pm 61	12.1
D	29	10.2	145	72	0.51	0.033	2.762 \pm 0.047	0.14696 \pm 0.00739	2.763 \pm 0.047	0.14667 \pm 0.00739	1991 \pm 29	2307 \pm 87	13.7
D	51	38.1	101	88	0.90	0.371	2.311 \pm 0.040	0.18841 \pm 0.00113	2.320 \pm 0.040	0.18510 \pm 0.00134	2311 \pm 34	2699 \pm 12	14.4
D	72	59.1	255	87	0.35	0.048	3.054 \pm 0.050	0.13802 \pm 0.00321	3.055 \pm 0.050	0.13759 \pm 0.00322	1825 \pm 26	2197 \pm 41	16.9
D	59	46.1	197	65	0.34	0.047	3.019 \pm 0.050	0.14245 \pm 0.00358	3.021 \pm 0.050	0.14204 \pm 0.00359	1843 \pm 27	2252 \pm 44	18.2
D	60	47.1	141	83	0.61	0.017	2.018 \pm 0.035	0.28703 \pm 0.02226	2.018 \pm 0.035	0.28688 \pm 0.02226	2594 \pm 37	3401 \pm 121	23.7
D	17	17.1	390	62	0.16	-0.013	3.881 \pm 0.062	0.12047 \pm 0.00446	3.881 \pm 0.062	0.12058 \pm 0.00446	1478 \pm 21	1965 \pm 66	24.8

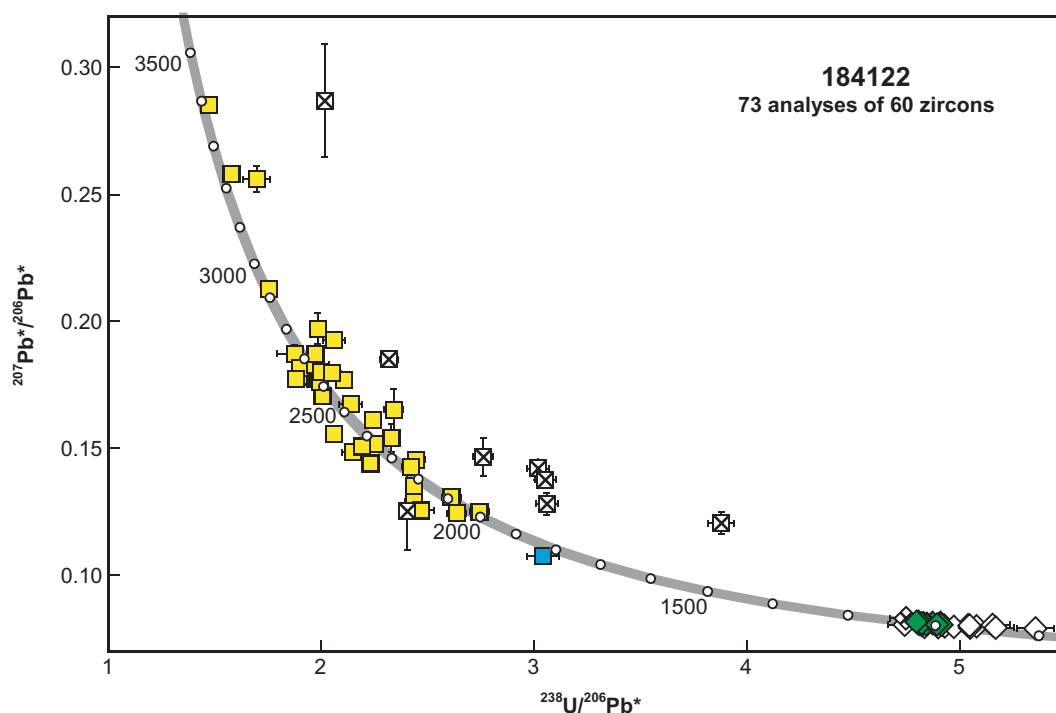


Figure 2. U-Pb analytical data for sample 184122: metamorphosed quartz sandstone, Plum Pudding Rocks. Green diamonds denote Group 1 (metamorphic zircon rims); blue square denotes Group 2 (youngest detrital zircon core); yellow squares denote Group 3 (older detrital zircon cores affected by minor ancient loss of radiogenic Pb); white diamonds denote Group 4 (metamorphic zircon rims affected by minor ancient loss of radiogenic Pb); crossed diamond denotes Group 5 (core-rim overlap); crossed squares indicate ungrouped analyses (discordance >10%)

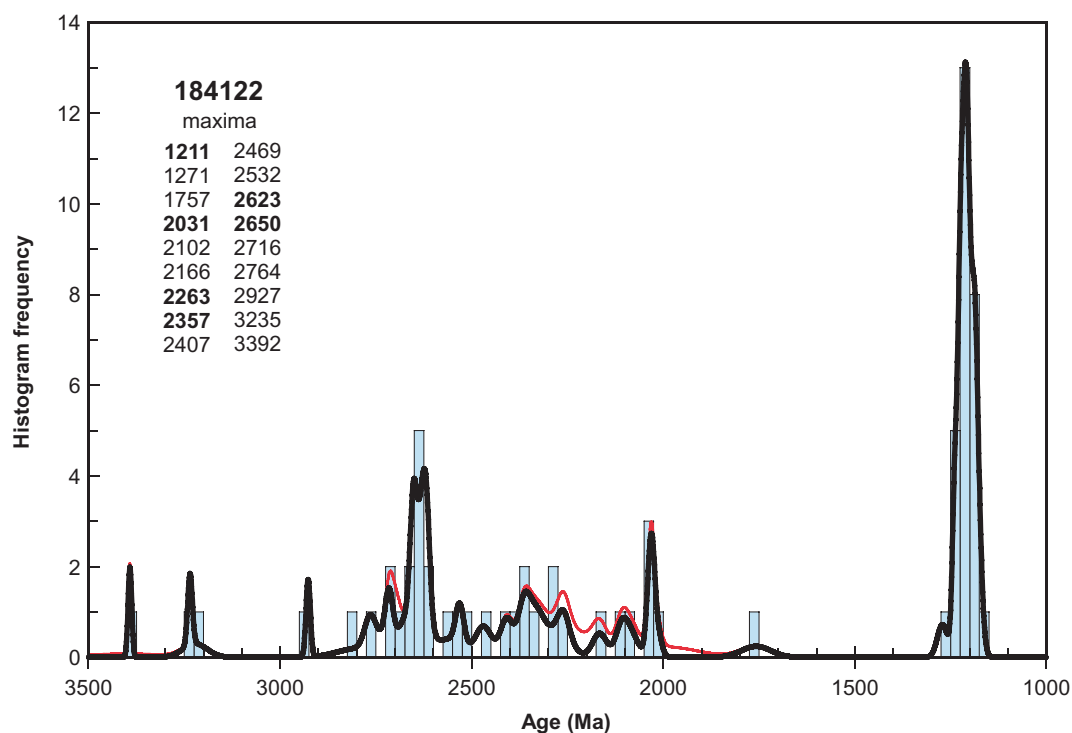


Figure 3. Probability density diagram and frequency histogram for sample 184122: metamorphosed quartz sandstone, Plum Pudding Rocks. Heavy curve, maxima values, and frequency histogram (bin width 25 Ma) include only data with discordance <10% (65 analyses of 54 zircons). Light curve includes all data (73 analyses of 60 zircons)

the monzogranite (GSWA 184123; Bodorkos and Wingate, 2008). This indicates that both rocks were metamorphosed during the same tectonothermal event, which corresponds to Stage II of the Albany–Fraser Orogeny (Clark et al., 2000).

References

- Bodorkos, S, and Clark, DJ, 2004, Evolution of a crustal-scale transpressive shear zone in the Albany–Fraser Orogen, SW Australia: 2. Tectonic history of the Coramup Gneiss and a kinematic framework for Mesoproterozoic collision of the West Australian and Mawson cratons: *Journal of Metamorphic Geology*, v. 22, p. 713–731.
- Bodorkos, S, and Wingate, MTD, 2008, 184123: garnet-bearing monzogranitic gneiss, Plum Pudding Rocks; Geochronology dataset 702, *in* Compilation of geochronology data: Geological Survey of Western Australia.
- Clark, DJ, Hensen, BJ, and Kinny, PD, 2000, Geochronological constraints for a two-stage history of the Albany–Fraser Orogen, Western Australia: *Precambrian Research*, v. 102, p. 155–183.
- Myers, JS, 1995, Geology of the Esperance 1:1 000 000 sheet: Western Australia Geological Survey, 1:1 000 000 Geological Series Explanatory Notes, 10p.
- Stacey, JS, and Kramers, JD, 1975, Approximation of terrestrial lead isotope evolution by a two-stage model: *Earth and Planetary Science Letters*, v. 26, p. 207–221.

Recommended reference for this publication

Bodorkos, S, and Wingate, MTD, 2008, 184122: metamorphosed quartz sandstone, Plum Pudding Rocks; Geochronology dataset 701, *in* Compilation of geochronology data: Geological Survey of Western Australia.

Data obtained:	21 September 2006
Data released:	31 July 2008
Updated:	30 June 2009